Volume 17 | Number 9 | September 2020

www.plasma-polymer

Check for updates

PLASMA PROCESSES AND POLYMERS

Investigation of air plasma generated by surface microdischarge for decellularized porcine aortic valve leaflets modification

Chen Lu, Jinchi Dai, Nianguo Dong, Yu Zhu, Zilan Xiong

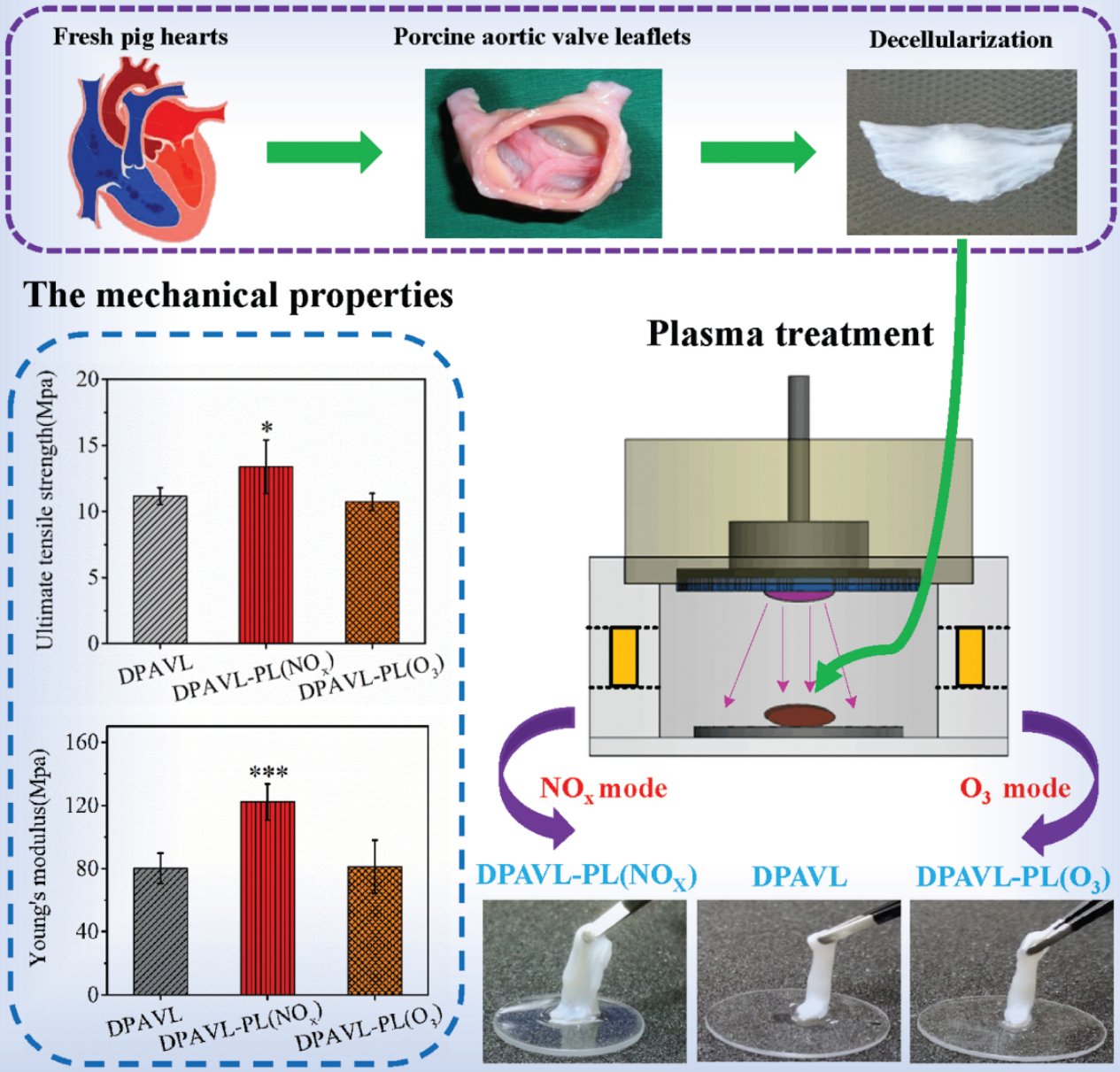

WILEY-VCH

Received: 9 May 2020 | Revised: 18 June 2020 | Accepted: 24 June 2020

DOI: 10.1002/ppap.202000100

COMMUNICATION

PLASMA PROCESSES AND POLYMERS

Investigation of air plasma generated by surface microdischarge for decellularized porcine aortic valve leaflets modification

Chen Lu[1] | **Jinchi Dai**[2] | **Nianguo Dong**[2] | **Yu Zhu** | **Zilan Xiong**[1]

[1]State Key Laboratory of Advanced Electromagnetic Engineering and Technology, Huazhong University of Science and Technology, Wuhan, Hubei, China

[2]Department of Cardiovascular Surgery, Union Hospital, Tongji Medical College, Huazhong University of Science and Technology, Wuhan, Hubei, China

Correspondence
Zilan Xiong, State Key Laboratory of Advanced Electromagnetic Engineering and Technology, Huazhong University of Science and Technology, Wuhan, 430074 Hubei, China.
Email: zilanxiong@hust.edu.cn

Funding information
National Natural Science Foundation of China, Grant/Award Number: 51907076

Abstract

In this study, the surface microdischarge (SMD) device was used to modify the mechanical properties of decellularized porcine aortic valve leaflets (DPAVL). It was found that SMD treatment under NO_x mode considerably improved the ultimate tensile strength and the Young's modulus of DPAVL, whereas treatment under O_3 mode had no effect. The absorbance band peak at ~1,375 cm^{-1}, measured by Fourier-transform infrared spectrometer, increased with treatment time in the freeze-dried DPAVL group under NO_x mode treatment. The microstructure was not destroyed and blood compatibility test showed no toxicity. The reaction between plasma-activated species and the DPAVL and the pH change, other than temperature/UV irradiation, plays a major role. All of the results indicate that cold atmospheric plasma treatment seems to be a potential alternative for DPAVL modification.

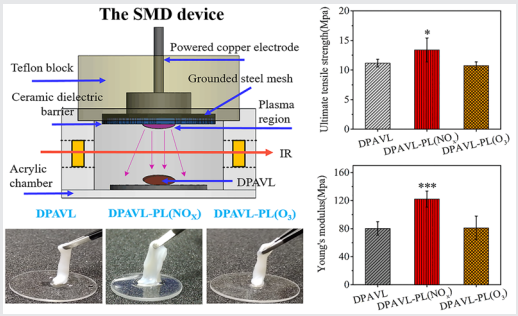

KEYWORDS

biomaterials, decellularized porcine aortic valve leaflet, dielectric barrier discharge, mechanical properties, modification

1 | INTRODUCTION

According to statistics, the incidence rate of valvular diseases in the United States is about 2.5%, of which the incidence rate for people over 75 years old is about 13.2%.[1] The root cause of valvular diseases is the abnormal shape of the heart valves, so the fundamental treatment for valvular diseases is heart valve replacement surgery, which is achieved by removing the diseased heart valves and replacing them with the prosthetic heart valves.[2] The most commonly used prosthetic heart valves are mechanical and bioprosthetic valves.[3] However, a common disadvantage of mechanical and bioprosthetic valves is that they are both nongrowing valves. With the development of regenerative medicine, tissue-engineered heart valves are expected to be a kind of

promising valve replacement.[4] Among them, decellularized valves have received extensive attention for their similar structure with the natural valves and low immunogenicity.[5] Nevertheless, there are still some issues of decellularized valves that need to improve. For example, the mechanical properties of the valve leaflets are important indicators to measure the performance of the decellularized valve, which is of great significance for clinical application.[6] The strength, durability, and flexibility of the decellularized valve may be reduced by poor mechanical properties of the valve, which contribute to calcification, mechanical fatigue, tissue degradation of the valve, and even clinical failure.[7,8]

Cold atmospheric plasmas (CAPs) have been widely used in the biomedical field in recent years.[9–15] Due to the high-energy charged particles, active oxides and nitrides, free radicals, electric fields, ultraviolet rays, and others, CAPs have been proved to be beneficial for disinfection,[16] wound treatment,[17] cancer treatment,[18] material modification,[19] stem cell differentiation,[20] cytoprotection,[21] and dentistry applications.[22] CAPs also have potential in tissue engineering and regenerative medicine.[23,24] CAP treatment under certain conditions can enhance the surface activity of biological functional materials without destroying the original structure and characteristics of biological materials, which makes it a competitive candidate in the field of biomedical tissue engineering.[25,26]

On the basis of the application defects of the existing decellularized porcine aortic valve leaflets (DPAVL), CAP generated by surface microdischarge (SMD) device was adopted here to treat the DPAVL. The sketch of SMD and the experimental setup is shown in Figure 1a. The powered electrode made of copper is 20 mm in diameter and 5 mm in thickness, covered by polytetrafluoroethylene for insulation shielding. A stainless steel woven wire mesh (wire diameter: 0.5 mm and the mesh density: 4×4 mesh/cm^2) is used as the ground electrode. A ceramic sheet (40 mm in diameter and 1 mm in thickness) is fixed between the copper sheet and the woven wire mesh. The SMD device was placed on the top of a cylindrical acrylic chamber (60 mm in diameter and 22 mm in height) during operation. During treatment, the DPAVL samples were placed on a circular quartz glass (30 mm in diameter and 1.2 mm in thickness), which was located at the bottom center of the cylindrical chamber. The distance between the ground electrode and the circular quartz glass was fixed at 15 mm. Two ZnSe windows were installed in the walls of the chamber for the Fourier-transform infrared spectroscopy (FTIR) measurements. An AC power supply (CTP-2000K; Corona Lab) was applied to generate the sinusoidal AC voltage with a specific peak-to-peak value and frequency.

Depending on the gas-phase product, the operating mode of the SMD device can be generally divided into NO_x mode and O_3 mode.[27] For the NO_x mode and O_3 mode, the dominating gas-phase product is mainly nitrogen oxides and O_3, respectively. In this study, both the NO_x mode and the O_3 mode were applied to treat the DPAVL. When operated in the NO_x mode, the peak-to-peak value of the applied voltage $V_{p\text{-}p}$ was fixed at 11 kV with a power density of ~1.767 W/cm^2. When operated in

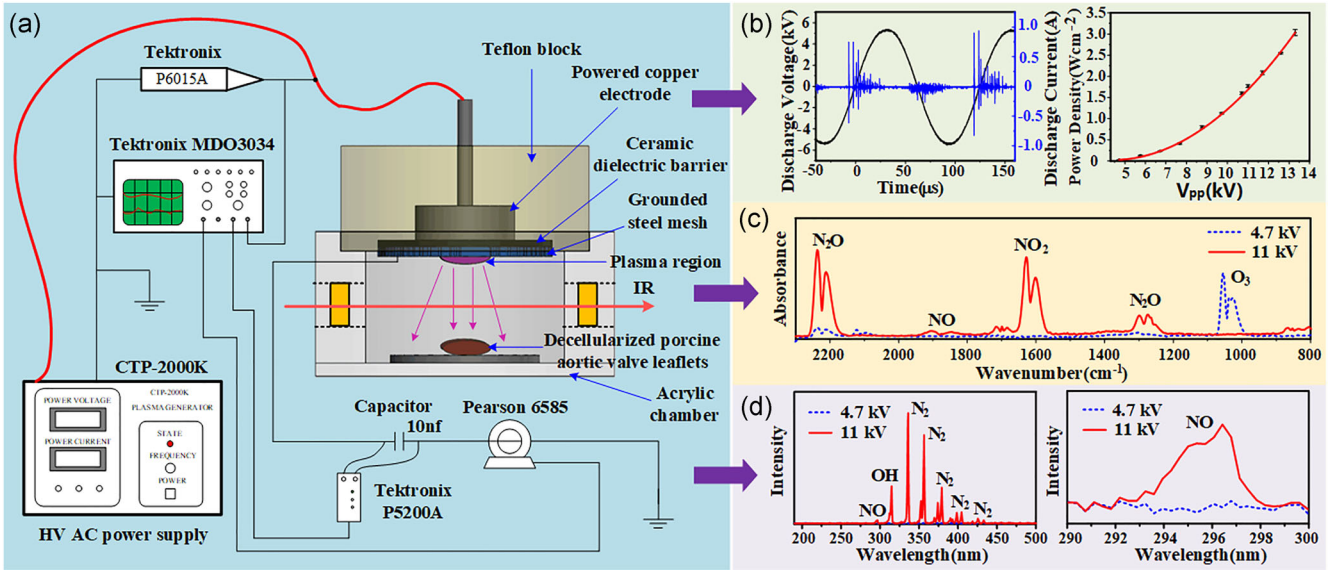

FIGURE 1 (a) The sketch of surface microdischarge (SMD) and the experiment setup. (b) The typical *U-I* waveform and the power consumption versus applied voltage. (c) The Fourier-transform infrared spectra of SMD operating in O_3 and NO_x mode at 4.7 and 11 kV, respectively. (d) The optical emission spectra of SMD operating in O_3 and NO_x mode

the O_3 mode, the peak-to-peak value of the applied voltage $V_{p\text{-}p}$ was fixed at 4.7 kV with a power density of ~0.027 W/cm^2. For all the experiments, the frequency was fixed at 8 kHz. The voltage and current waveforms were recorded and the power density was calculated by using the Lissajous method (seen in Figure 1b). The qualitative analysis of the gas-phase products was conducted by Fourier-transform infrared spectrometer (VERTEX 70; Bruker), seen in Figure 1c. The gas-phase products are different in the NO_x mode and O_3 mode, which are similar to those in other reported studies. Figure 1d shows the optical emission spectrum (OES; FLAME-S-UV-VIS-ES; Ocean Optics). The results of OES also confirms the existence of NO in the gas phase and the difference between the O_3 and NO_x mode.

Fresh hearts of adult pigs were harvested from a local slaughtering factory. A total of 240 porcine aortic valve leaflets used in this investigation were obtained from over 80 pigs. The dissection of porcine aortic valve leaflets and decellularization procedures used here is similar to that reported in Qiao et al.[7] After washing with phosphate-buffered saline (PBS), the DPAVL were stored at 4°C in PBS for use. The DPAVL treatment processes by SMD device are as follows: (a) a piece of DPAVL is randomly taken out from the pre-prepared samples, and one side of the selected sample is placed at the bottom center of the cylindrical chamber. The specified sinusoidal AC voltage is turned on to generate plasma, and the DPAVL is treated in the chamber for 12 min. (b) The AC power supply is shut down after 12 min and the selected sample is taken out. The electrodes and the cylindrical chamber are cooled simultaneously. (c) The other side of the selected sample is placed at the bottom center of the cylindrical chamber after the electrodes and the cylindrical chamber are sufficiently cooled. The treatment process in Step (a) is repeated. (d) The AC power supply is shut down after another 12 min and the selected sample is taken out. The electrodes and the cylindrical chamber are cooled again before the next treatment.

The DPAVL treated following the above procedure under the NO_x mode of SMD were marked as DPAVL-PL(NO_x), and the DPAVL treated following the above procedure under the O_3 mode of SMD were marked as DPAVL-PL(O_3). For each treatment condition, at least six samples were repeated. After treatment, the samples were put into PBS and stored at 4°C for other measurements.

The mechanical properties of the DPAVL, DPAVL-PL(NO_x), and DPAVL-PL(O_3) were tested by the electronic mechanical testing machine (CMT 2102) after treatment. The mechanical test method is similar to that reported in Liu et al.,[28] and the results are shown in Figure 2. Young's modulus is a physical quantity describing the deformation resistance of a solid material, which can be obtained by measuring the slope of the stress–strain curve in the high-strain region. As can be seen from Figure 2a, the overall mechanical properties of the DPAVL-PL(NO_x) are improved. The ultimate tensile strength and the Young's modulus of the DPAVL, DPAVL-PL(NO_x), and DPAVL-PL(O_3) are compared in Figure 2b,c. The ultimate tensile strength and the Young's modulus of the DPAVL-PL(NO_x) were increased by 19.98% and 52.15%, compared with that of the untreated DPAVL, respectively. However, the results in DPAVL-PL(O_3) group basically remain the same as the DPVAL, which indicates that SMD in the O_3 mode has no effect on the properties of DPAVL.

To find out why the SMD treatment in NO_x mode could effectively improve the mechanical properties of DPAVL, the possible factors related to the process such as temperature, UV irradiation, and pH were all tested. The

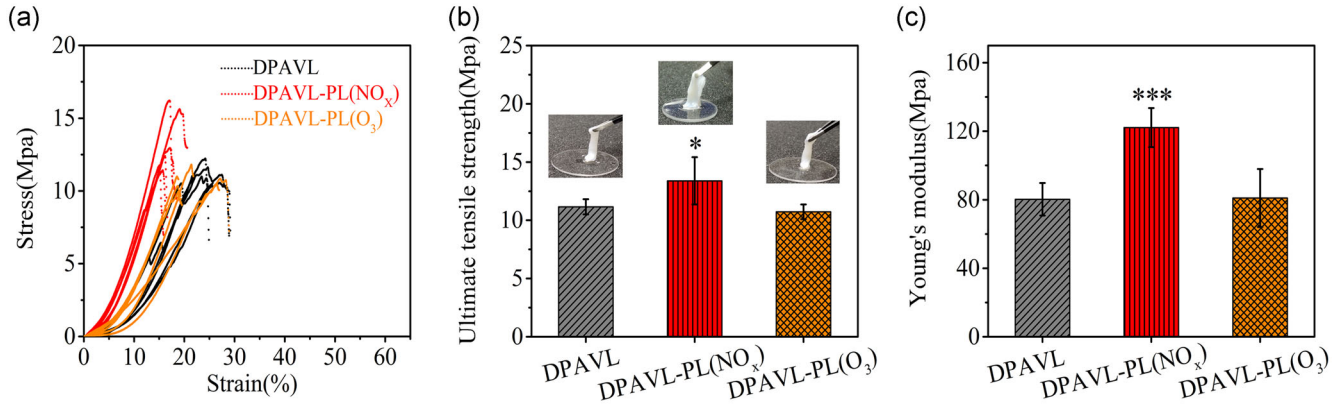

FIGURE 2 The mechanical property results of the DPAVL, DPAVL-PL(O_3), and DPAVL-PL(NO_x). (a) The overall mechanical properties of the three groups. (b) The ultimate tensile strength of the three groups. (c) Young's modulus of the three groups. Data are expressed as mean values ±*SD*; $n = 6$. *$p < .05$, ***$p < .0005$, compared with untreated DPAVL. DPAVL, decellularized porcine aortic valve leaflets; *SD*, standard deviation

average temperature inside the treatment chamber under the NO_x mode was measured as ~20°C; therefore, to determine the role of temperature, the DPVAL were tested at an ambient temperature of 20°C for 24 min. To analyze the role of UV irradiation, a piece of quartz sheet was located directly above the chamber to prevent the plasma-activated species to act with the DPVAL, and then the DPAVL were treated under the same conditions as the DPAVL-PL(NO_x). The results in Figure 3 show that the temperature and UV irradiation have no effect on the mechanical properties of the DPVAL, which also illustrates that the temperature and UV irradiation are not responsible for the improvement of mechanical properties.

As it is known, there are various active species in the gas phase created by SMD in the NO_x mode. When they come in contact with water, the pH will decrease to some value and form plasma-activated water. The pH value on the DPAVL-PL(NO_x) surface was measured as ~6; therefore, to determine the role of pH, the DPVAL were tested in dilute nitric acidic solutions (HNO_3) with pH 3 and pH 6 for 12 min. As can be seen in Figure 4, the dilute acidic solution of pH 3 and pH 6 can slightly improve the mechanical properties of the DPAVL, but the values of ultimate tensile strength and the Young's modulus are obviously lower than those of the DPAVL-PL(NO_x), which also indicates that the pH may contribute to a part of the effect. Also, it is observed that low pH or longtime treatment using acid will cause serious dehydration of the DPAVL.

One of the other possible reasons is the reaction between the plasma-active species in the NO_x mode and the DPAVL materials. Attenuated total reflection Fourier-transform infrared spectroscopy was used to check the functional group change on the surface of the DPAVL after SMD treatment in both the NO_x and O_3 mode, as can be seen in Figure 5. Some pronounced absorbance bands can be identified: the amide A band in the vicinity of 3,300 cm^{-1} (νNH), the amide B band in the vicinity of 3,100 cm^{-1} (νNH), the amide I band in the vicinity of 1,640 cm^{-1} (νCO), the amide II band in the vicinity of 1,550 cm^{-1} (δNH), and the amide III band in the vicinity of 1,240 cm^{-1} (νCN).[29] In this test, samples of freeze-dried DPAVL were used. An absorbance band peak at ~1,375 cm^{-1} in the freeze-dried DPAVL-PL is steadily enhanced with treatment time in the NO_x mode, as seen in the zoomed FTIR results in Figure 5b,ii. However, this absorbance band is not enhanced in the freeze-dried DPAVL-PL(O_3), even for a longer treatment time.

To check the surface morphology change of the DPAVL, scanning electron microscopy (SEM; JSM-6510; Japan Electronics Co., Ltd.) was applied, and the experimental method is similar to that reported in Liu et al.[28] The SEM images of the DPAVL-PL(NO_x) and DPAVL are shown in Figures 6a,i and 6a,ii, respectively. The results show that there is no significant difference in the microstructure between the DPAVL-PL(NO_x) and DPAVL. Meanwhile, some gas-phase products of SMD under the NO_x mode are toxic, such as nitric oxide, nitrogen dioxide, and so on. It is necessary to check whether the treated DPAVL are safe for clinical application. To verify the toxicity of the DPAVL-PL(NO_x), the blood compatibility test was carried out as follows: (a) both DPAVL and DPAVL-PL(NO_x) were sterilized with 75% alcohol and then rinsed in PBS three times, 5 min each time. (b) DPAVL, DPAVL-PL(NO_x), and negative control were immersed in 1-ml normal saline, the positive control was immersed in 1-ml distilled water, and each group was preheated at 37°C for 30 min. (c) Each group was added with 0.5-ml fresh human blood donated by healthy volunteers and incubated at 37°C for 60 min. As can be seen in Figure 6b,i–iv, no significant hemolysis is found in the DPAVL-PL(NO_x), compared with the negative control.

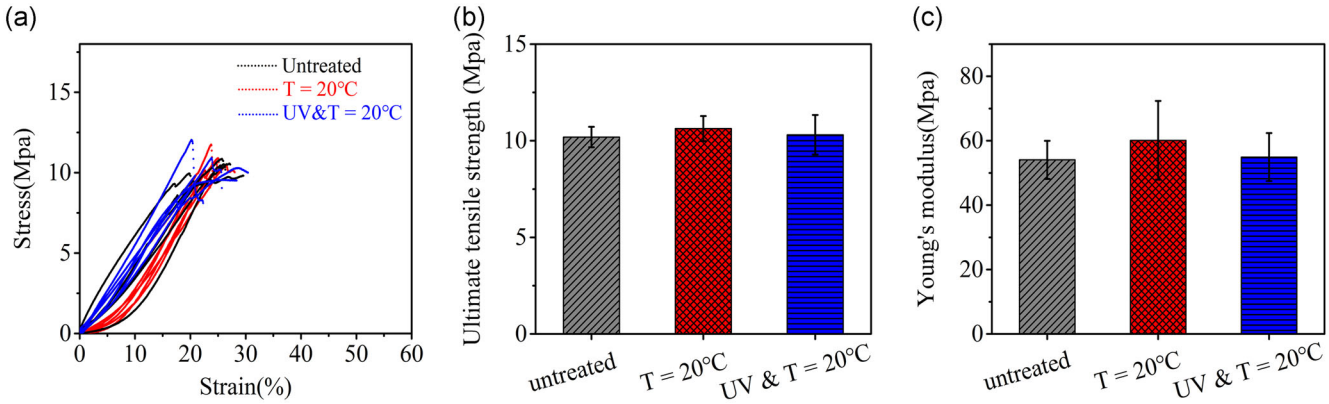

FIGURE 3 (a) The overall mechanical properties. (b) The influence of temperature and UV radiation on the ultimate tensile strength. (c) The influence of temperature and UV radiation on Young's modulus. Data are expressed as mean values ± standard deviation; $n = 6$. $p > .05$, compared with untreated decellularized porcine aortic valve leaflets

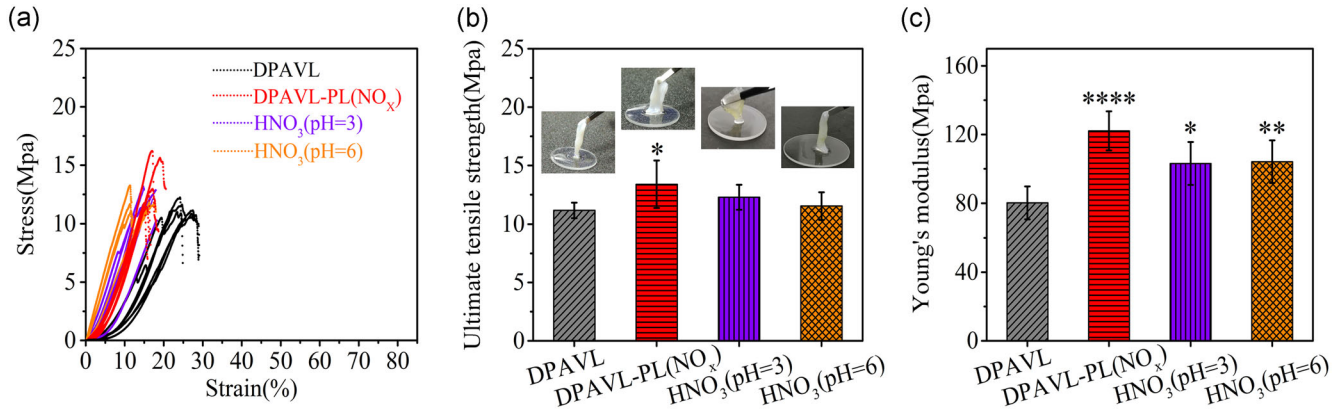

FIGURE 4 The mechanical properties of the DPAVL, DPAVL-PL(NO_x), and DPAVL treated by a dilute nitric acid solution with pH 3 and pH 6. (a) The influence of pH on the overall mechanical properties of the DPVAL. (b) The influence of pH on the ultimate tensile strength. (c) The influence of pH on Young's modulus. Data are expressed as mean values ±*SD*; $n = 6$. *$p < .05$, **$p < .01$, ****$p < .0001$, compared with DPAVL. DPAVL, decellularized porcine aortic valve leaflets; *SD*, standard deviation

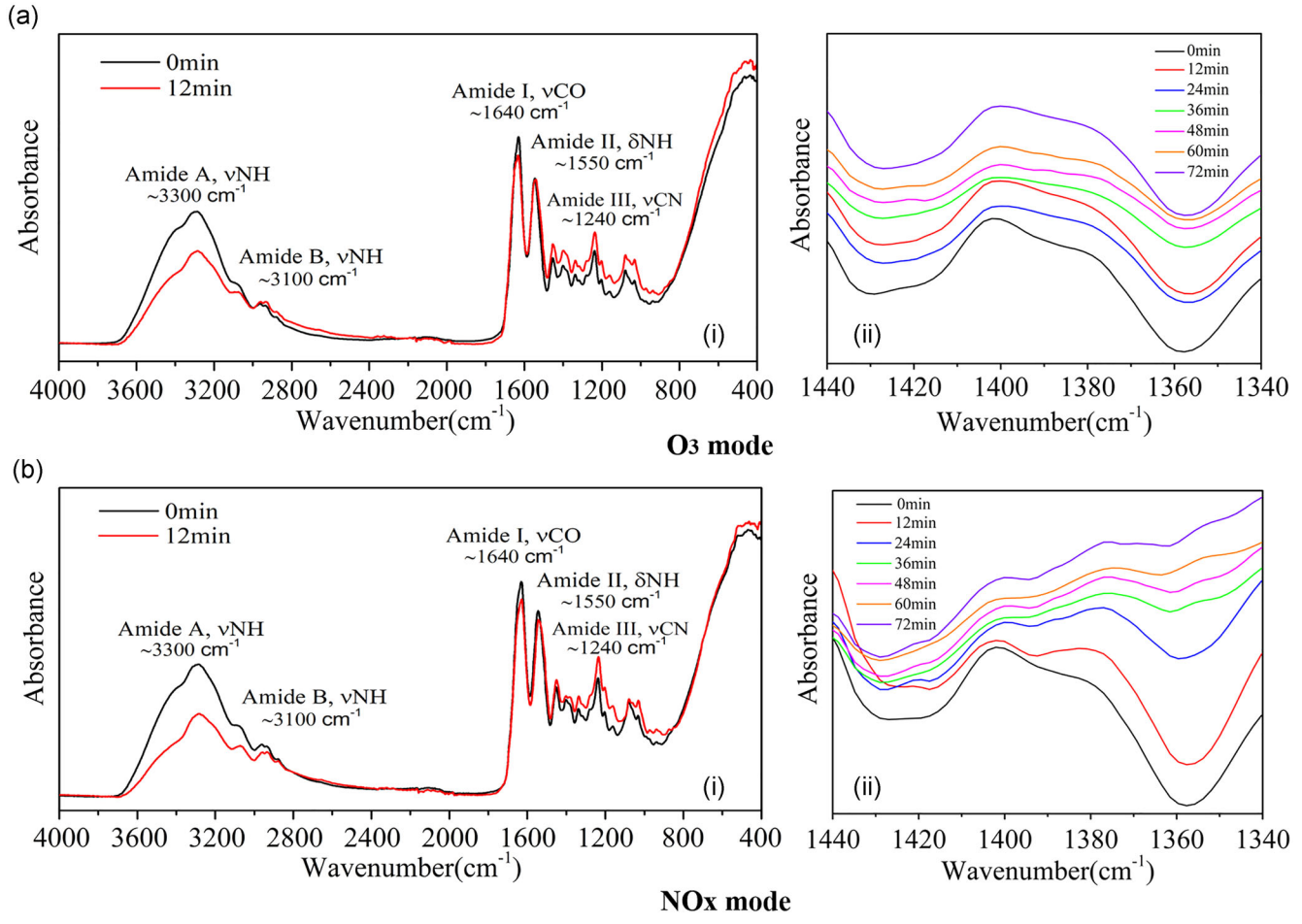

FIGURE 5 The infrared absorption spectra of the freeze-dried decellularized porcine aortic valve leaflets (DPAVL). (a) Fourier-transform infrared (FTIR) spectra of the freeze-dried DPAVL-PL (O_3). (b) FTIR spectra of the freeze-dried DPAVL-PL(NO_x). (a,i) The spectra in the 400–4,000 cm^{-1} of the freeze-dried DPAVL-PL(O_3). (a,ii) The spectra in the 1,340–1,440 cm^{-1} of the freeze-dried DPAVL-PL(O_3). (b,i) The spectra in the 400–4,000 cm^{-1} of the freeze-dried DPAVL-PL(NO_x). (b,ii) The spectra in the 1,340–1,440 cm^{-1} of the freeze-dried DPAVL-PL(NO_x)

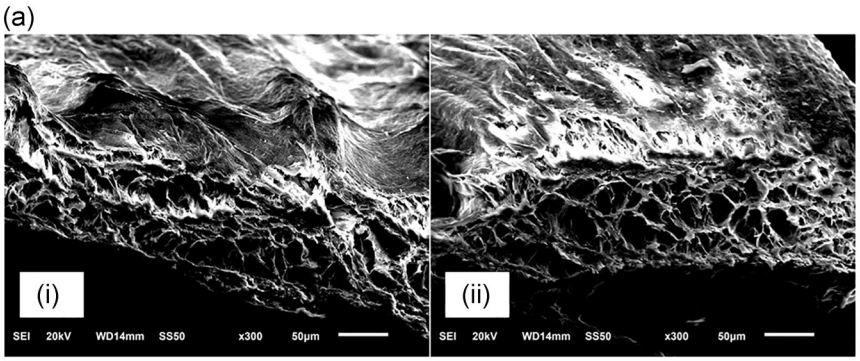

The SEM images of the DPAVL and DPAVL-PL (NO_X)

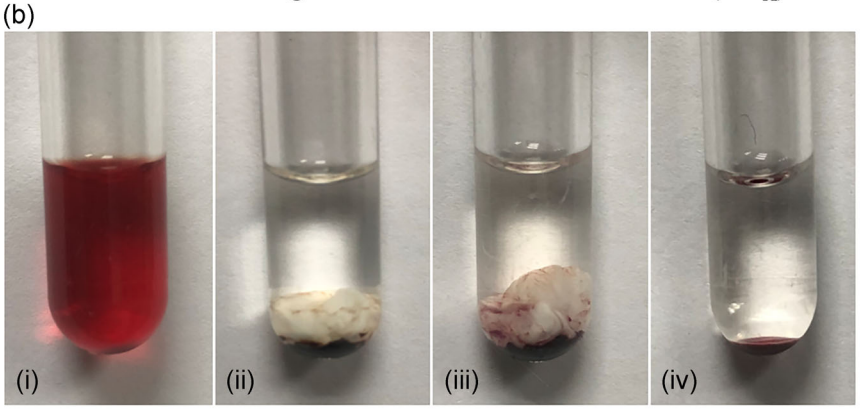

The results of blood compatibility of the DPAVL and DPAVL-PL (NO_X)

FIGURE 6 (a) The scanning electron microscopy (SEM) images of decellularized porcine aortic valve leaflet (DPAVL) and DPAVL-PL (NO_x); (b) the results of blood compatibility test. The amplification of the SEM is 300. (a,i) shows the SEM images of DPAVL. (a,ii) shows the SEM images of DPAVL-PL (NO_x). (b,i–iv) show the hemolysis results of the positive control (the hemolysis rate is high), DPAVL, DPAVL-PL(NO_x), and the negative control (the hemolysis rate is low), respectively

In this study, the SMD device was used to treat DPAVL and was shown to be a good method to enhance the mechanical properties. The ultimate tensile strength and the Young's modulus of DPAVL-PL(NO_x) were considerably improved as compared with the untreated sample, whereas there was no difference after SMD treatment in the O_3 mode. Temperature and UV irradiation did not affect the mechanical properties of DPVAL during SMD treatment. However, surface reaction and pH may be two of the main factors. The microstructure of the DPAVL was not destroyed and the toxic component of DPAVL-PL(NO_x) was low after SMD treatment. In conclusion, CAPs treatment may be a potential alternative for the modification of the biological heart valve for clinical application. Further works such as condition optimization, cell adhesion test, and animal test need to be conducted in the future.

ORCID

Zilan Xiong http://orcid.org/0000-0003-1095-3959

REFERENCES

[1] E. J. Benjamin, P. Muntner, A. Alonso, M. S. Bittencourt, C. W. Callaway, A. P. Carson, A. M. Chamberlain, A. R. Chang, S. Cheng, S. R. Das, F. N. Delling, L. Djousse, M. Elkind, J. F. Ferguson, M. Fornage, L. C. Jordan, S. S. Khan, B. M. Kissela, K. L. Knutson, T. W. Kwan, D. T. Lackland, T. T. Lewis, J. H. Lichtman, C. T. Longenecker, M. S. Loop, P. L. Lutsey, S. S. Martin, K. Matsushita, A. E. Moran, M. E. Mussolino, M. O'Flaherty, A. Pandey, A. M. Perak, W. D. Rosamond, G. A. Roth, U. Sampson, G. M. Satou, E. B. Schroeder, S. H. Shah, N. L. Spartano, A. Stokes, D. L. Tirschwell, C. W. Tsao, M. P. Turakhia, L. B. VanWagner, J. T. Wilkins, S. S. Wong, S. S. Virani, *Circulation* **2019**, *139*, 56.

[2] K. Nishimura, *J. Am. Coll. Cardiol.* **2014**, *63*, 57.

[3] M. K. Sewell-Loftin, Y. W. Chun, Ali Khademhosseini, W. D. Merryman, *J. Cardiovasc. Transl. Res.* **2011**, *4*, 658.

[4] C. V. C. Bouten, A. Driessen-Mol, F. P. T. Baaijens, *Expert Rev. Med. Devices* **2012**, *9*, 453.

[5] A. Neumann, S. Cebotari, I. Tudorache, A. Haverich, S. Sarikouch, *Biomed. Tech.* **2013**, *58*, 453.

[6] J. Liao, E. M. Joyce, M. S. Sacks, *Biomaterials* **2008**, *29*, 1065.

[7] W. Qiao, P. Liu, D. Hu, M. A. Shirbini, X. Zhou, N. Dong, *J. Tissue Eng. Regener. Med.* **2018**, *12*, e828.

[8] W. Sun, M. Sacks, G. Fulchiero, J. Lovekamp, N. Vyavahare, M. Scott, *J. Biomed. Mater. Res.* **2004**, *69*, 658.

[9] J. Kaupe, C. T. Tschang, F. Birk, D. Coenen, M. H. Thoma, S. Mitic, *Plasma Processes Polym.* **2019**, *16*, e1800196.

[10] D. B. Graves, *Phys. Plasmas* **2014**, *21*, 080901.

[11] Z. Xiong, Q. Huang, Z. Wang, X. Lu, Y. Pan, *IEEE Trans. Plasma Sci.* **2013**, *41*, 1746.

[12] G. Neretti, F. Tampieri, C. A. Borghi, P. Brun, R. Cavazzana, L. Cordaro, E. Marotta, C. Paradisi, P. Seri, M. Taglioli,

B. Zaniol, M. Zuin, E. Martines, *Plasma Processes Polym.* **2018**, *15*, e1800105.
[13] F. Yue, S. Mohades, M. Laroussi, X. Lu, *IEEE Trans. Plasma Sci.* **2016**, *44*, 2754.
[14] J. Ma, H. Zhang, C. Cheng, J. Shen, L. Bao, W. Han, *Plasma Processes Polym.* **2016**, *14*, 1600162.
[15] M. Laroussi, X. Lu, M. Keidar, *J. Appl. Phys.* **2017**, *122*, 020901.
[16] Z. Xiong, D. B. Graves, *J. Phys. D: Appl. Phys.* **2017**, *50*, 1.
[17] G. Daeschlein, M. Napp, S. von Podewils, S. Lutze, S. Emmert, A. Lange, I. Klare, H. Haase, D. Gümbel, T. von Woedtke, M. Jünger, *Plasma Processes Polym.* **2014**, *11*, 175.
[18] X. Xu, X. Dai, L. Xiang, D. Cai, S. Xiao, K. Ostrikov, *Plasma Processes Polym.* **2018**, *15*, e1800052.
[19] Y. Kusano, A. Bardenshtein, P. Morgen, *Plasma Processes Polym.* **2017**, *15*, e1700131.
[20] S. Zhao, R. Han, Y. Li, C. Lu, X. Chen, Z. Xiong, X. Mao, *J. Appl. Phys.* **2019**, *125*, 163301.
[21] X. Yan, Z. Meng, J. Ouyang, Y. Qiao, J. Li, M. Jia, F. Yuan, K. Ostrikov, *J. Phys. D: Appl. Phys.* **2018**, *51*, 1.
[22] M. Gherardi, R. Tonini, V. Colombo, *Trends Biotechnol.* **2018**, *36*, 583.
[23] N. Chernets, J. Zhang, M. J. Steinbeck, D. S. Kurpad, E. Koyama, G. Friedman, T. A. Freeman, *Tissue Eng., Part A* **2015**, *21*, 300.
[24] I. Trizio, F. Intranuovo, R. Gristina, G. Dilecce, P. Favia, *Plasma Processes Polym.* **2015**, *12*, 1451.
[25] O. Karaman, S. Kelebek, E. A. Demirci, F. İbiş, M. Ulu, U. K. Ercan, *Tissue Eng. Regener. Med.* **2018**, *15*, 13.
[26] M. Wang, X. Cheng, W. Zhu, B. Holmes, M. Keidar, L. G. Zhang, *Tissue Eng., Part A* **2014**, *20*, 1060.
[27] M. J. Pavlovich, D. S. Clark, D. B. Graves, *Plasma Sources Sci. Technol.* **2014**, *23*, 065036.
[28] C. Liu, W. Qiao, H. Cao, J. Dai, F. Li, J. Shi, N. Dong, *Biomater. Sci.* **2020**, *8*, 2549.
[29] A. V. Rivera, H. Oldenhof, A. Hilfiker, W. F. Wolkers, *Spectrochim. Acta A* **2019**, *214*, 95.

How to cite this article: Lu C, Dai J, Dong N, Zhu Y, Xiong Z. Investigation of air plasma generated by surface microdischarge for decellularized porcine aortic valve leaflets modification. *Plasma Process Polym*. 2020;17:e2000100.
https://doi.org/10.1002/ppap.202000100